Combustion Science and Technology

ISSN: (Print) (Online) Journal homepage: https://www.tandfonline.com/loi/gcst20

An Experimental Investigation of Supersonic Combustion of Mildly Cracked N-Dodecane

Naifu Cui, Wei Rao, Yujun Li, Taichang Zhang & Xuejun Fan

To cite this article: Naifu Cui, Wei Rao, Yujun Li, Taichang Zhang & Xuejun Fan (2022): An Experimental Investigation of Supersonic Combustion of Mildly Cracked N-Dodecane, Combustion Science and Technology, DOI: 10.1080/00102202.2022.2135096

To link to this article: https://doi.org/10.1080/00102202.2022.2135096

COMBUSTION SCIENCE AND TECHNOLOGY
https://doi.org/10.1080/00102202.2022.2135096

Taylor & Francis
Taylor & Francis Group

An Experimental Investigation of Supersonic Combustion of Mildly Cracked N-Dodecane

Naifu Cui[a], Wei Rao[b], Yujun Li[a,c], Taichang Zhang[a,c], and Xuejun Fan[a,c]

[a]State Key Laboratory of High Temperature Gas Dynamics, Institute of Mechanics, Chinese Academy of Sciences, Beijing, China; [b]State Key Laboratory of Laser Propulsion & Application, Department of Aerospace Science and Technology, Space Engineering University, Beijing, China; [c]School of Engineering Science, University of Chinese Academy of Sciences, Beijing, China

ABSTRACT

In this paper, a novel two-stage hydrocarbon fuel heating and delivery system was used to more accurately simulate the state of fuel in the cooling channel of the regenerative cooling engine. Mildly cracked (<10%) experiments of *n*-dodecane were conducted by using the new heating system and pyrolysis products were sampled and analyzed. The ignition delay time and laminar flame speed of the cracked products were different from those of the surrogate gas fuel. When the temperature is 1100 K, the ignition delay time of the cracked products are ~50% higher than that of surrogate gas fuel. The laminar flame speed of the cracked products is about 30% lower than that of surrogate gas fuel at the equivalence ratio of 1.0. The supersonic combustion experiments of mildly cracked and different equivalence ratios *n*-dodecane were also employed at Mach number 3.0 of the isolator entrance, with total temperature ~1550 K and total pressure ~1.5 MPa. The static pressure along the axis of combustor was measured, while the velocity and temperature of the airflow at the exit of combustor were also measured by the tunable diode laser absorption spectroscopy (TDLAS). The distributions of airflow velocity, static temperature, and total temperature along the combustor at different conditions were analyzed through a one-dimensional analysis method. The deviations of velocity and temperature of the airflow are less than 4% and −6%, respectively, which indicates the calculation is in great accordance with the TDLAS detections. The experimental data will be helpful for validating the simulation of supersonic combustion, and studying the influence of mildly cracked fuel on supersonic combustion characteristics.

ARTICLE HISTORY
Received 2 August 2022
Revised 8 October 2022
Accepted 9 October 2022

KEYWORDS
Mildly cracked; n-dodecane; supersonic combustion; regenerative cooling

Introduction

The regenerative cooling is an effective way to solve the problems induced by the high thermal loads during the operation of scramjets. When the liquid hydrocarbon fuel is used to regeneratively cool the scramjet, it will absorb much more heat from the combustor wall with Mach number increasing, thereby vary from the liquid state to the supercritical state, and eventually to the cracked state. When the fuel temperature increases above 800 K, it begins to crack. Moreover, the pressure in the cooling channel generally exceeds 3 MPa, higher than the critical pressure of hydrocarbon fuel. Therefore, it is of great significance to

CONTACT Taichang Zhang taichang@imech.ac.cn State Key Laboratory of High Temperature Gas Dynamics, Institute of Mechanics, Chinese Academy of Sciences, Beijing 100190, China

understand the influence of the cracked hydrocarbon fuels on the supersonic combustion performance.

The decomposition reactions and conversion rate of hydrocarbon fuel dramatically change with fuel temperature, residence time, and cracking type. Consequently, the compositions and properties of cracked hydrocarbon fuel will vary at practical cracking conditions, which will affect the subsequent combustion process (Gascoin, Abraham, and Gillard 2010; Wang, Guo, and Lin 2009; Xian et al. 2010; Zhong et al. 2009). In addition, the components of the cracked hydrocarbon fuel are too complex to be accurately measured. The combustion intensity and efficiency of cracked kerosene, as well as the effect of cracked kerosene on self-ignition were studied by simulating the cracking state of kerosene in the regenerative cooling engine channel through a home-made kerosene heating system (Fan et al. 2007). The results show that thermally cracked kerosene significantly improved the combustion intensity and efficiency, and the amount of pilot hydrogen required for achieving self-ignition decreased with an increasing extent of kerosene cracking. Yu et al. (2006) experimentally studied the effects of entry static pressure, injection scheme, entry Mach number, and combustor entry geometry on the combustion performance of pyrolysis kerosene. The results show that the jet penetration depths of kerosene with different cracking degrees were basically similar at the tested conditions. Ravindran et al. (2019) used numerical methods to investigate the mixing characteristics of the uncracked fuel and cracked fuel compositions and found that mixing benefits were gained by injecting cracked hydrocarbon fuels compared to heavy uncracked fuels. The decreased stagnation pressure losses of injecting cracked hydrocarbon fuels enhanced the overall scramjet performance for the given fuel system pressure and temperature. However, the jet penetration decreases as the cracking extent increases.

In recent years, considering the complex composition of kerosene, ethylene, or a mixture of ethylene and methane as the surrogate gas fuel have been basically used instead of the cracked hydrocarbon fuel (Gallo et al. 2015; Huang et al. 2018; Huang, Sobel, and Spadaccini 2002; Ma, Zhong, and Zhang 2018; Nakaya et al. 2019; Sun et al. 2015; Zhong et al. 2019). Gokulakrishnan et al. (2016) found that increasing the H_2 or C_2H_4 fraction in the binary mixture of C_3H_6 reduced the ignition delay time linearly. Increasing H_2 or C_2H_4 in the binary mixtures of C_2H_6 had little effect on the ignition delay time. Shin and Sung (2018) applied a RANS/LES framework to analyze supersonic combustion characteristics of a surrogate fuel in a model scramjet combustor. The surrogate of pyrolysis kerosene was composed of ethylene and methane. The flame of surrogate fuel was more vulnerable to quenching and flame quenching occurred in the immediate vicinity of the injector. Denman et al. (2017) performed experiments with and without hydrogen-pilot to study ignition and combustion. At equivalence ratio of 0.3 of pilot hydrogen, the surrogate gas fuel burnt vigorously and a high-pressure rise was noted in the entire engine flow path. Nakaya et al. (2015) studied different ratios of hydrogen, methane, ethane, and ethylene according to the content of hydrogen and small molecule hydrocarbons (less than 3 carbon atoms) in the surrogate fuel. The ignition characteristics results show that ignitions for ethylene could be observed at a stagnation temperature of 1800 K, on the other hand, ignitions for methane and ethane could be observed above a stagnation temperature of 2200 K, respectively. In addition, it was found that ethylene had a promoting effect and methane had an inhibitory effect on the flame stabilization.

It can be concluded that the mixture composition and proportion of the small molecule of cracked gas have a significant impact on supersonic ignition and flame stabilization. When the hydrocarbon fuel is largely cracked, it is basically a mixture of small molecules. But when the hydrocarbon fuel is mildly cracked, it needs to be verified whether the law obtained by the surrogate gas fuel study is applicable. In the literature, the combustion properties of mildly cracked hydrocarbon fuels are rarely introduced, and the influence mechanism of the small amount of pyrolysis components on the supersonic combustion of the entire fuel is rarely analyzed.

In this paper, the mildly cracked experiments of *n*-dodecane were conducted under the pressure range of 3.0–6.5 MPa and the temperature range of 830–920 K, and the components of cracked products under different conditions were analyzed. The ignition delay time and laminar flame speed of the mildly cracked products and commonly used surrogate gas fuel in the literature were calculated and compared, and it was found that the results of these two kinds of fuels were significantly different. Therefore, it is necessary to study the supersonic combustion characteristics of mildly cracked products under real condition. Then, supersonic combustion experiments of mildly cracked products at fuel temperature between 860 K and 880 K, different pressures, and different equivalence ratios were conducted under the fixed condition of combustor entrance with Mach number 3.0, total temperature ~1550 K, and total pressure ~1.5 MPa. The airflow velocity and temperature at the exit of the combustor were measured by TDLAS, and compared with the one-dimensional calculation results. The accuracy of the measured data is verified, which is helpful for the further numerical simulation of supersonic combustion of mildly cracked fuel.

Experimental system

All experiments were conducted at the Institute of Mechanics, Chinese Academy of Sciences. Cracked fuel was obtained by using a novel two-stage hydrocarbon fuel heating and delivery system. Supersonic combustion experiments of cracked fuel were performed at a direct-connect supersonic combustion facility with the fuel heating system. The airflow velocity and temperature at the combustor exit were measured by the tunable diode laser absorption spectroscopy (TDLAS), which was developed by the Space Engineering University and suitable for the measurement of the supersonic combustion. These experimental devices are described below, respectively.

Direct-connect supersonic combustion facility

The direct-connect supersonic combustion facility is composed of an air heater, an equipment nozzle, and a model combustor. The operation and data acquisition of the whole experiment can be displayed in real time and controlled by a computer. The vitiated air, which is supplied by burning H_2 in air with oxygen replenishment, has a stagnation temperature range of 420–2200 K and a stagnation pressure range of 0.3–4.5 MPa. The high-enthalpy flow passes through a replaceable and two-dimensional converging-diverging Laval nozzle and then enters the rectangular supersonic model combustor with the entrance cross section of 50 mm (height) × 70 mm (width).

The Laval nozzle is adopted to accelerate the high-enthalpy vitiated air flow to designed supersonic flow, which is Mach number of 3.0 in this work. The schematic diagram of the

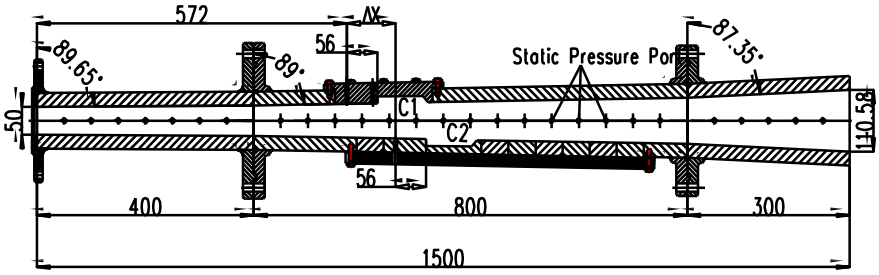

Figure 1. Schematic diagram of model combustor.

combustor is shown in Figure 1, the isolation section is 400 mm long with an expansion angle 0.7 deg, the combustion section is 800 mm long with an expansion angle 2.0 deg, and the expansion section is 300 mm long with an expansion angle 5.3 deg. The upstream cavity (C1) and the downstream cavity (C2) integrated fuel-injection/flame-holder are installed on the opposite sides of the combustor. The spacing ΔX between two fuel injectors is variable in the range of 40–390 mm through varying the relative location of C1 and C2. ΔX is 90 mm in this work. The two cavities have a depth of 12 mm, and the cavity aft ramp angle and L/D ratio are 45 deg and 7, respectively. The distance between the upstream injection position of fuel and the isolator entrance is 572 mm, and the downstream injection position of fuel is 662 mm from the isolator entrance. The upstream and downstream fuel injectors have two orifices with the diameter of 2 mm, respectively. The distance between the cavity upstream transverse fuel injection ports and the cavity leading edge is 56 mm, respectively. The pilot hydrogen is injected from five orifices of 1 mm diameter. The distance between the upstream pilot hydrogen injection ports and the cavity leading edge is 8 mm. Fuel and hydrogen are injected into supersonic airstream vertically and then ignited by a spark plug of 50 J/pulse energy at the bottom of upstream cavity.

The stagnation pressure and temperature of the vitiated airflow are measured by using a CYB-10S pressure transducer with an accuracy of 0.1% and a type-B thermocouple, respectively. A Motorola MPX22000 pressure sensor is installed on the side wall of the combustor to measure the wall static pressure. The measurement points are arranged at intervals of 50 mm from entrance to exit of the combustor, and 27 measurement points are arranged on each side. The mass flow rate of the gas flows (air, hydrogen, and oxygen) was controlled and measured by sonic flowmeters. The mass flow rate coefficients of the sonic nozzles were calibrated with an uncertainty less than 1%.

Fuel pyrolysis experiment facility

In order to simulate the state of hydrocarbon fuel in the cooling channel of regenerative cooling combustor, a novel two-stage hydrocarbon fuel heating and delivery system was designed, as shown in Figure 2. The first stage in the system adopts a manner of heat storage, which can heat hydrocarbon fuel of ~12 kg to 570 K with negligible coking deposits, and the second stage adopts a manner of heat sink, which can heat the high-temperature fuel output from the first stage to a desired temperature (below 1000 K) about 0.1 s. In addition, the second stage has 18 fuel channels in the heat sink block. The

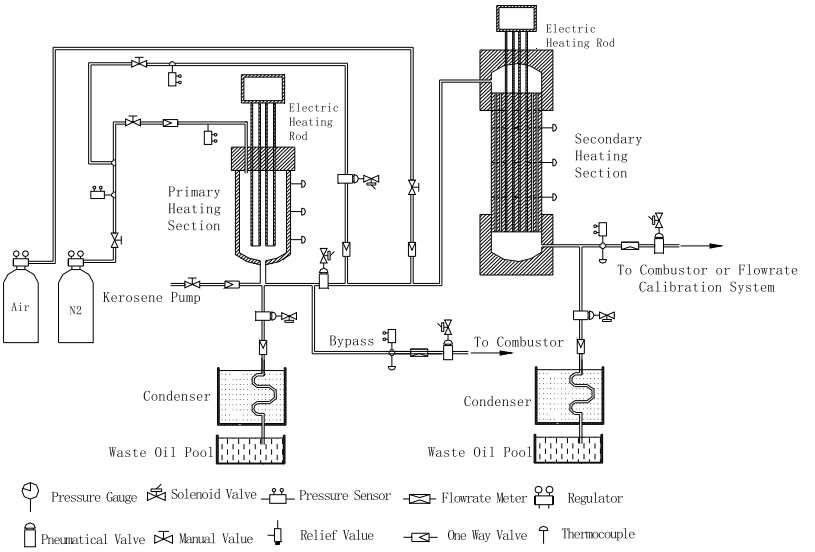

Figure 2. Schematic of two-stage heating system of hydrocarbon fuel.

diameter and length are 2.0 mm and 1000 mm of the fuel channel, respectively. It can simulate the fuel in the channel of scramjet combustor. This heating system provided cracked fuel in the temperature range of 880 ± 20 K and the pressure range of 3.0–6.0 MPa for this experiment.

In the current investigation, the hydrocarbon fuel was pumped into the primary heating section before each test. Two pneumatic valves are installed at the exit of the primary heating section and the secondary heating section respectively to turn on/off fuel transportation. When the fuel reach designed temperature at a given pressure in the primary heating section, the high-temperature fuel is extruded to the secondary heating section by nitrogen, and the fuel is heated to the required temperature in a very short time before being injected into the model combustor. Three K-type thermocouples are installed on the outer surfaces of the two heating sections from top to bottom, which are used to achieve real-time monitoring and heating feedback control of the temperature of each heating section. Since the thermal isolation of the two-stage kerosene heating system was so good, it took more than 24 h to cool down to the room temperature. To remove coking in the experiments, a small flowrate of airflow was introduced into the second stage after experiments.

The collection of cracked products and flow rate calibration system was shown in Figure 3. The flow rate of mildly cracked *n*-dodecane was controlled by a sonic flowmeter installed at the exit of the heating system. The cracked products were condensed by cooling water after passing through the sonic flowmeter. The liquid products and carbon deposits (if present) were collected directly after cooling and the gaseous products were collected using a container immersed in a water pool, and the mixture volume was measured by the volume of water displaced. The composition of the cracked gas and its percentages and average molecular weights were obtained by gas chromatographic (GC-MS QP2010 ultra) analysis. The previous experimental results show that the sonic flowmeter can control the flow accurately (Fan et al. 2006). During the combustion experiment, the flow rate of cracked

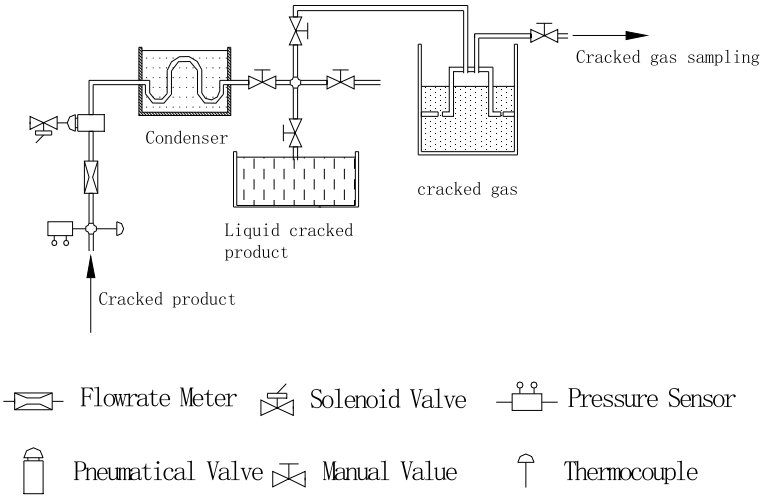

Figure 3. Schematic of cracked product collection system.

n-dodecane can be adjusted by changing the fuel pressure which is measured immediately upstream the throat of the sonic flowmeter.

TDLAS system

The TDLAS system mainly includes three parts: the photoelectric signal acquisition module, the laser probe array, and the data processing software. The schematic diagram is shown in Figure 4. In this study, the laser probe array is mounted on the adapter frame, which is installed at the exit of the model combustor. The laser probe array is further divided into

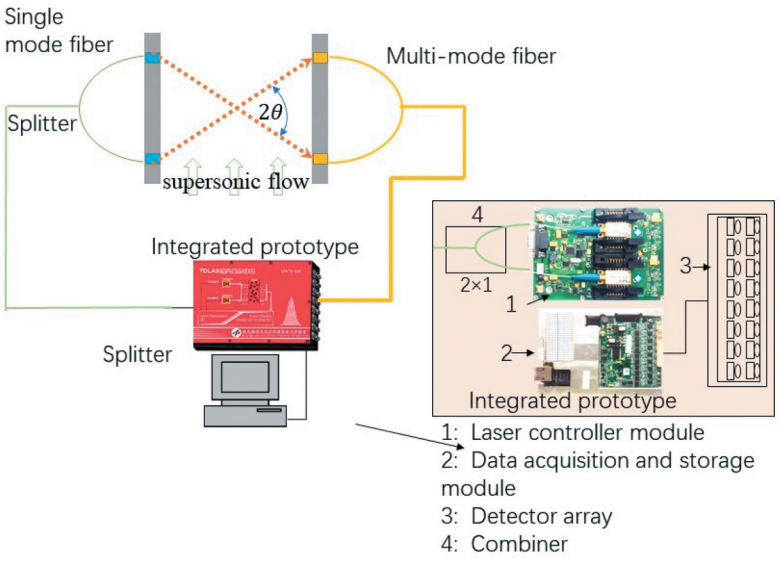

Figure 4. Schematic diagram of TDLAS system.

a laser transmitting probe and a laser receiving probe, and the two correspond to each other in quantity and position. The arrangement of the probe array is determined by the size of the probe and the size of the measured physical parameters. Schematic diagram of TDLAS system as shown in Figure 4. The signal processing software mainly complete the TDLAS signal demodulation and calculate the physical parameters such as temperature and airflow velocity.

Results and discussions

Pyrolysis experiments

This paper mainly focuses on the supersonic combustion of mildly cracked *n*-dodecane at fuel temperature between 860 K and 880 K, different pressures, and different equivalence ratios. Therefore, the composition of cracked products in the pressure range of 3.0–6.5 MPa, and the temperature range of 830–920 K as shown Table 3 were analyzed. Figure 5 shows the normalized results of mass flow rate per unit throat area of sonic flowmeter (Q/A*) in the fuel temperature range of 830–920 K for a fixed fuel pressure of 3.5 MPa as the work published before (Fan et al. 2007). The sonic flowmeter with throat diameters of 2.8 mm was employed in the pyrolysis and combustion experiments.

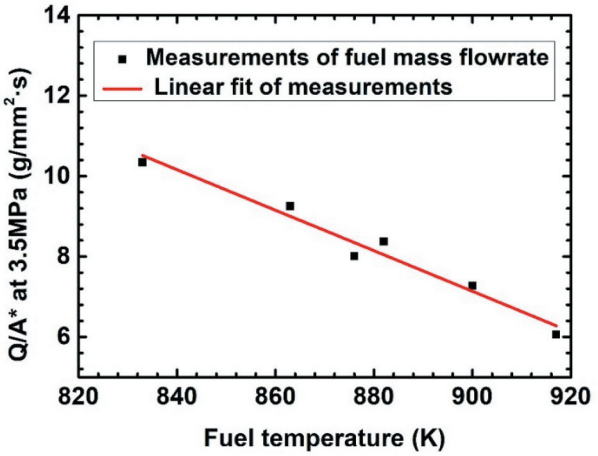

Figure 5. Fuel cracking flowrate under different conditions and its linear fitting.

Table 1. Compositions of cracked gas.

		MF mol%		
Species	Formula	2#	3#	4#
Hydrogen	H_2	2.90	2.80	3.9
Methane	CH_4	19.8	20.7	18.6
Ethylene	C_2H_4	28.9	27.0	31.7
Ethane	C_2H_6	21.8	21.6	20.5
Propene	C_3H_6	15.4	17.0	15.1
Propane	C_3H_8	11.2	10.9	10.2

Table 2. Components of cracked products of liquid.

		WF wt%		
Species	Formula	2#	3#	4#
1-Heptene	C_7H_{14}	1.38	2.42	2.46
1-Octene	C_8H_{16}	1.38	2.74	2.48
1-Nonene	C_9H_{18}	1.36	2.64	2.36
1-Decene	$C_{10}H_{20}$	1.58	2.51	2.40
N-dodecane	$C_{12}H_{26}$	94.3	89.6	90.3

Table 3. Experimental conditions of cracked n-dodecane.

Cracked experiment No.	T_F K	p_F MPa	Q_F g/s	Q/A* at 3.5MPa g/mm^2·s
1#	833	3.94	71.7	10.3
2#	863	3.87	63.0	9.3
3#	876	5.75	81.0	8.0
4#	882	3.94	58.0	8.4
5#	900	3.95	50.5	7.3
6#	917	3.96	42.2	6.1

Table 1 demonstrates that the main components of cracked gas under different conditions are hydrogen, methane, ethane, ethylene, propane, and propylene. Table 2 demonstrates that the main components of the liquid cracked products are *n*-dodecane, 1-heptene, 1-octene, and 1-nonene. The results also indicate that when the temperature between 860 K and 880 K, the compositions of the cracked products are not significantly distinct under different conditions. The mass percentage deviation of the main components of the liquid cracked products is less than 5%, and that of the cracked gas is less than 14%. It can be concluded that the pressure has little effect on the cracking degree within this pressure range.

Ignition delay time and laminar flame speed

Jetsurf mechanism (Sirjean et al. 2008) was used to calculate the laminar flame speed and ignition delay time of the mildly cracked *n*-dodecane (4#) and surrogate gas fuel in the literature, in order to understand their combustion characteristics. Table 4 shows the compositions of fuels in the calculation. The temperature range of 1100–1600 K, and the pressure of 0.3 MPa were used in the calculation.

The results of ignition delay time and laminar flame speed show an obvious difference between surrogate gas fuel and mildly cracked products. Figure 6 indicates that the difference of ignition delay time among fuels is obvious in the temperature range of 1100–1600 K. So the ignition delay time is more sensitive to distinct components of fuels.

Table 4. Fuel components in the calculation.

	Fuel composition (by Volume)							
No.	$C_{12}H_{26}$	H_2	CH_4	C_2H_4	C_2H_6	C_3H_6	C_3H_8	Note
A	0.6	0.02	0.07	0.12	0.08	0.06	0.05	Cracked products(4#)
B	0	0.04	0.18	0.31	0.21	0.15	0.11	Cracked gas
C	0	0.06	0.29	0.41	0.24	0	0	Surrogate gas fuel (Nakaya et al. 2015)
D	1	0	0	0	0	0	0	N-dodecane

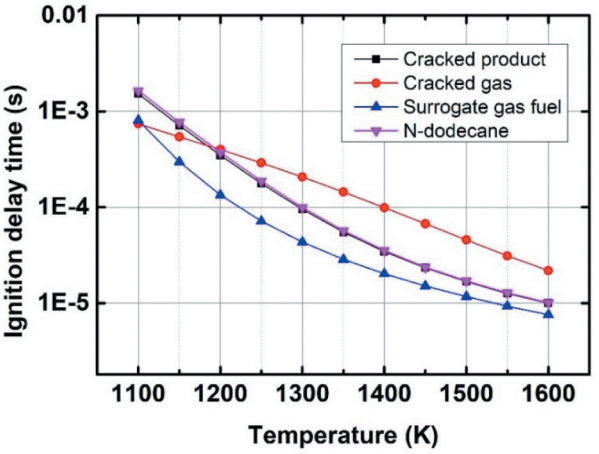

Figure 6. Ignition delay time of different fuels varies with temperature.

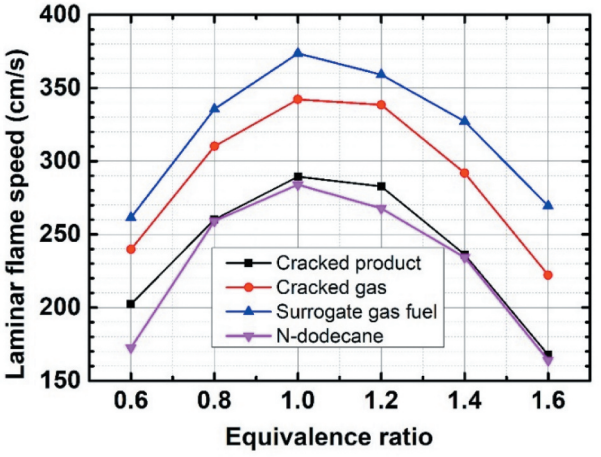

Figure 7. Laminar flame speed of different fuels at different equivalence ratios.

The ignition delay time of the surrogate gas fuel is relatively short, and that of the fuel increased when the large molecule hydrocarbons are contained. When the temperature is 1100 K, the ignition delay time of the cracked products are ~50% higher than that of surrogate gas fuel. Figure 7 demonstrates that the laminar flame speed of the cracked products is lower than that of surrogate gas fuel, and the difference is about 30% when the equivalence ratio is 1.0. Therefore, the supersonic combustion characteristics of surrogate gas fuel are not accurate to represent that of cracked products, and it is necessary to study the supersonic combustion characteristics of cracked products at low pyrolysis degrees.

Supersonic combustion

In this paper, in order to study the supersonic combustion performance of mildly cracked *n*-dodecane, a novel two-stage hydrocarbon fuel heating and delivery system was used to simulate the combustor wall channel of regenerative cooling engine, and to mildly crack *n*-dodecane. Then, experimental study of supersonic combustion characteristics of mildly cracked *n*-dodecane at different equivalence ratios were conducted. The distributions of the total temperature, static temperature, and airflow velocity along the axis of the combustor were calculated by one-dimensional analysis method according to the static pressure data from the combustion experiments. At the same time, TDLAS was used to measure the temperature and velocity of the airflow at the exit of the combustor. The accurate experimental data are helpful for the further numerical simulation of supersonic combustion of mildly cracked fuel.

The supersonic combustion experiments of three equivalence ratios were conducted under the condition of stable air flow, and the total air flowrate was ~1.0 kg/s. The pressure upstream the sonic flowmeter of pilot hydrogen, the fuel injection pressure, and the total pressure of the vitiated air are shown in Figure 8. As shown in Figure 8, the entire period can be divided into four periods, namely S1, S2, S3, and S4. In the period of S1, only the airflow is existed; in the period of S2, pilot hydrogen is burnt alone; in the period of S3, pilot hydrogen and fuel are burnt together, and in the period of S4, the fuel is burnt alone. It indicates that pilot hydrogen and fuel are injected into the combustor at different times in the stabilization time range of the total pressure. Figure 9 presents stable total temperature of the airflow.

According to the parameters shown in Table 5, mildly cracked *n*-dodecane at different equivalence ratios were injected into the model combustor. The distributions of static pressure in the periods of S1 (baseline) and S4 along the combustor wall at different equivalence ratios with combustion are shown in Figure 10. Flow separation of airflow without combustion (baseline) occurs in this work because the airflow pressure at the exit of the combustor is lower than the back pressure of 0.1 MPa, so the extrapolation of isentropic expansion is used for the baseline at the expansion section, as well as for the static pressure between 1450 and 1550 mm. The calculation uses the equations as below:

$$\frac{A}{A^*} = \frac{1}{M}\sqrt{\left[\frac{2\left(1+\frac{\gamma-1}{2}M^2\right)}{\gamma+1}\right]^{\frac{\gamma+1}{\gamma-1}}} \tag{1}$$

$$\frac{p_s}{p^*} = \left[\frac{\gamma+1}{2\left(1+\frac{\gamma-1}{2}M^2\right)}\right]^{\frac{\gamma}{\gamma-1}} \tag{2}$$

$$\frac{A_x}{A_1} = \frac{M_1}{M_x}\sqrt{\left[\frac{1+\frac{\gamma-1}{2}{M_x}^2}{1+\frac{\gamma-1}{2}{M_1}^2}\right]^{\frac{\gamma+1}{\gamma-1}}} \tag{3}$$

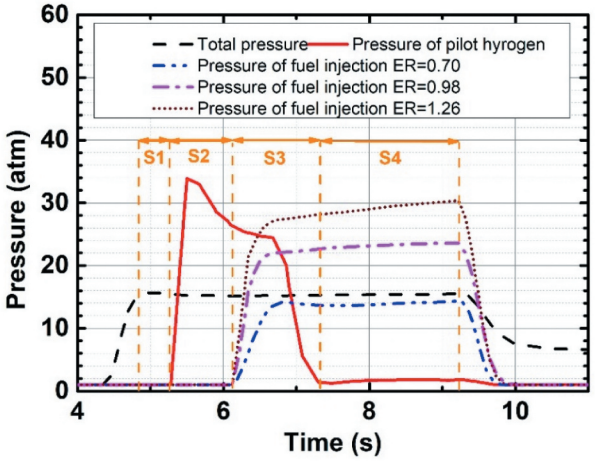

Figure 8. Total pressure of airflow, the pressures of pilot hydrogen and fuel.

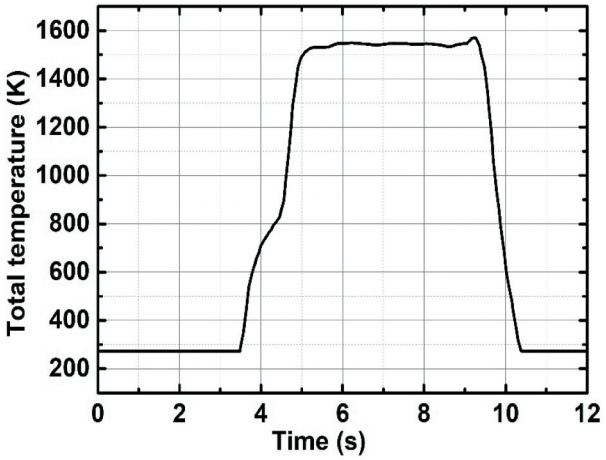

Figure 9. Total temperature of the vitiated inlet airflow.

Table 5. Experiment conditions of supersonic combustion.

	Conditions of flow										
Experiment No.	T_0 K	p_0 MPa	Q_{Air} kg/s	O_2 mol%	H_2O mol%	p_F MPa	T_F K	p_{inj} MPa	Q/A* at 3.5MPa g/mm^2·s	Q_F g/s	ER
SC1	1546	1.53	1.03	21.0	15.1	3.27	866	1.39	8.9	51.0	0.70
SC2	1546	1.53	1.03	21.0	15.1	4.84	875	2.32	8.4	71.7	0.98
SC3	1546	1.53	1.03	21.0	15.1	6.43	880	2.95	8.1	92.0	1.26

$$\frac{p_{Sx}}{p_{S1}} = \left[\frac{1+\frac{\gamma-1}{2}M_1{}^2}{1+\frac{\gamma-1}{2}M_x{}^2}\right]^{\frac{\gamma}{\gamma-1}} \tag{4}$$

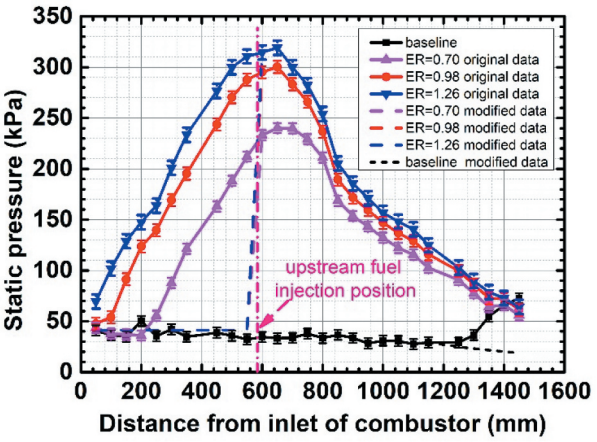

Figure 10. Static pressure distributions along the axis of combustor at different equivalence ratios.

In which, A is cross-sectional area,A^* is throat area, A_1 is cross-sectional area of entrance of the expansion section, M is Mach number of airflow, M_1 is Mach number of airflow at entrance of the expansion section, γ is the specific heat ratio,$p_s$is the static pressure,p_{s1} is the static pressure at entrance of the expansion section, $p^*$is the pressure of the throat. According to the configuration of the combustor, the M_x can be calculated by the above-mentioned Equations (1) and (3) then the p_{sx} can be calculated by the above-mentioned Equations (2) and (4). The result is shown in Figure 10. It indicates that the peak pressure on the wall of the combustor increases with the increase of the equivalence ratio of the cracked fuel, and the peak pressure appears at the same position around 640 mm from the entrance of the combustor. The static pressure reaches maximum near the position of fuel injection.

The rise of static pressure leads to the separation of the boundary layer, and the separation propagates upstream and downstream of the combustor along the subsonic region of the boundary layer. The expansion of the cross-sectional area of the combustor accelerates the supersonic airflow continuously, and cause static pressure to drop. With the increase of the equivalence ratio, the position where the static pressure begins to rise

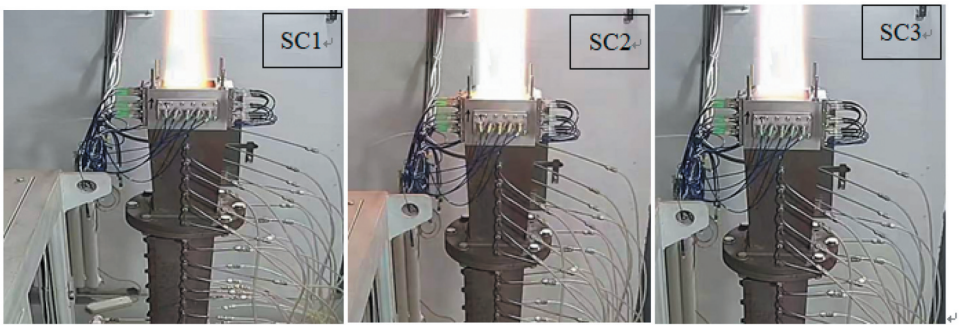

Figure 11. Flame imagines at the combustor exit.

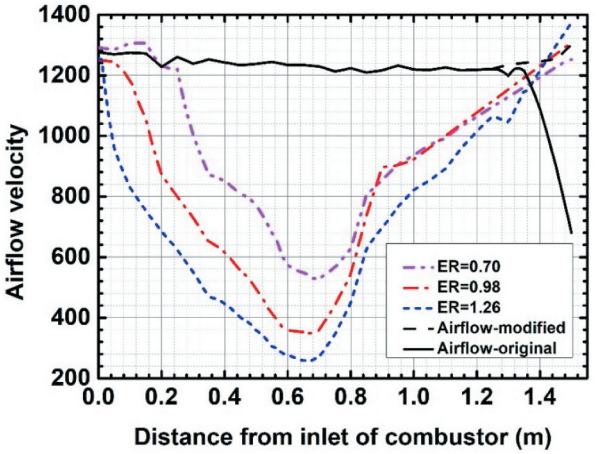

Figure 12. Distributions of airflow velocity at different equivalence ratios.

approaches the entrance of the combustor. Figure 11 indicates that the flames at the exit of the combustor have good uniformity.

The static pressures as shown above were used as the known conditions in a one-dimensional analysis method to calculate the aerodynamic parameter distributions along the combustor, such as distributions of velocity of airflow, static temperature, and total temperature. The friction coefficient $C_f$is obtained by the Reynolds similarity criterion. Figure 12 shows that the velocity distribution in the combustor with combustion at different equivalence ratios, as well as without combustion. For the original condition without combustion, the airflow velocity drops significantly from 1240 m/s to about 600 m/s due to the remarkable flow separation at the combustor exit. In the contrast, the modified velocity rises slightly in the expansion section of the combustor due to the increase of the cross-sectional area. The modified result is the velocity of the core flow without the influence of flow separation. With the increase of the equivalence ratios, the degree of air velocity reduction in the isolator gradually increases since the increase of heat release downstream enhances the shockwave train, while the airflow velocity reaches the minimum around the cavity and then accelerates with the increase of the cross-sectional area of the combustion section and the expansion section of the combustor.

As shown in Figure 10, the static pressure rises from the inlet of isolator to the upstream fuel injection location, which is due to the shock train in the isolation section rather than the combustion. It leads to unreal distributions of the airflow static temperature and total temperature along the axial direction in the isolator calculated by using the one-dimensional analysis method. In order to exclude the influence of the shock train on the distributions of the static temperature and total temperature, the static pressure of combustor inlet is instead for the static pressures between the isolator entrance and the upstream fuel injection position (the following is noted with "modified data"). Taking the equivalence ratio of 0.98 as an example, both the measured static pressure (original data) and the static pressure obtained by modified (modified data) as shown in Figure 10 were used to calculate the distributions of the static temperature and total temperature, which are

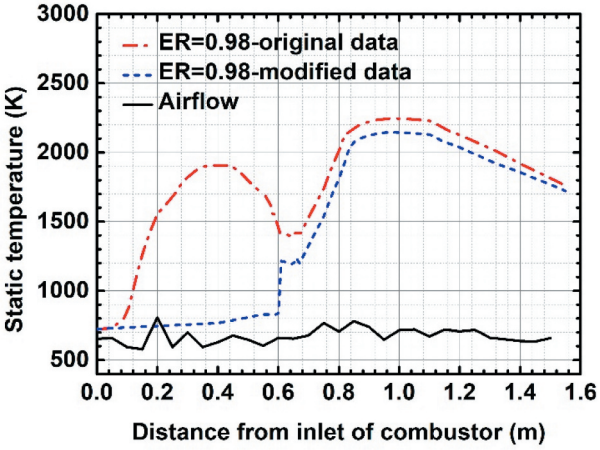

Figure 13. Static temperature distributions along the axis of combustor of original and modified data at equivalence ratio 0.98.

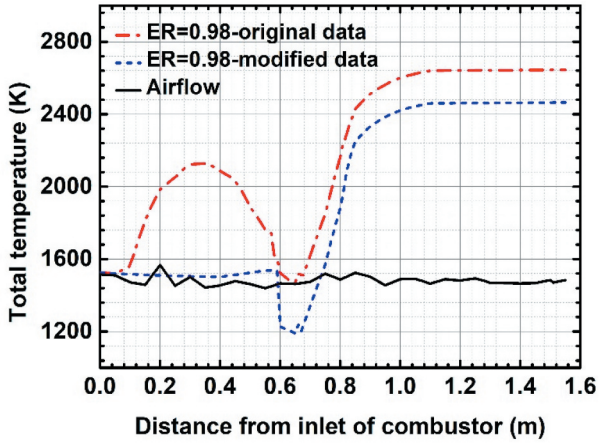

Figure 14. Total temperature distributions along the axis of combustor of original and modified data at equivalence ratio 0.98.

shown in Figures 13 and 14, respectively. The real distribution of static temperature and total temperature should be amongst these two conditions. It can be seen from the results that the difference under these two conditions in the section from the upstream fuel injection position to the combustor exit with combustion is less than 100 K. The difference of two conditions at different equivalence ratios are presented in the "belt form" in Figures 15 and 16.

Figures 15 and 16 show that the static temperature and total temperature, respectively. Two-staged fuel injections locate at 0.57 m and 0.66 m distances from the entrance of combustor. The two flame-holder cavities are 56 mm downstream of the fuel injections. The combustion occurs in the range of 0.57–0.90 m, so both the static temperature and the total temperature rise quickly. As shown in Figure 12, this region has a relatively low flow

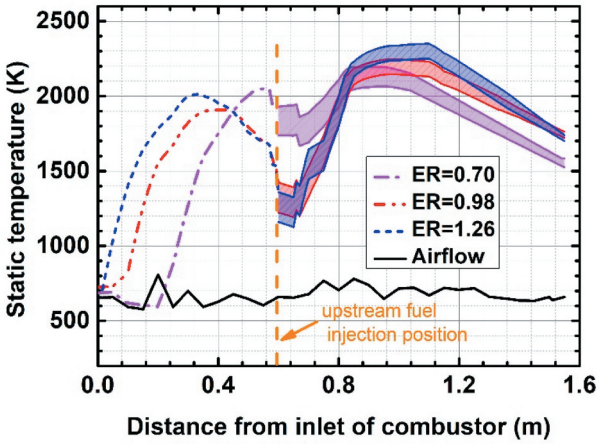

Figure 15. Distributions of airflow total temperature at different equivalence ratios.

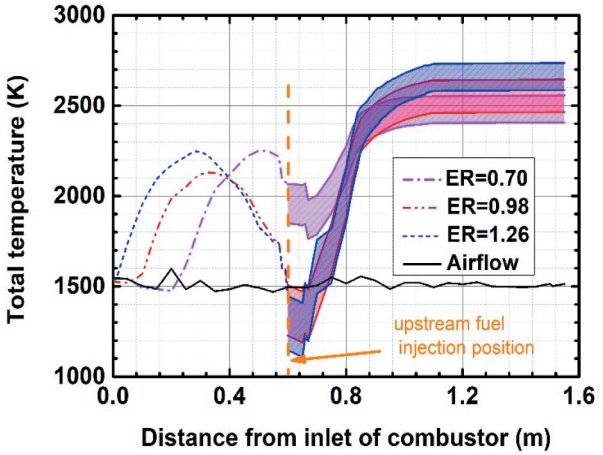

Figure 16. Distributions of airflow total temperature at different equivalence ratios.

velocity, which is conducive to the mixing and combustion of fuel and air to release greater heat. Then, a larger subsonic region is further formed, so the fuel burnt abundantly in the subsonic flow. From the results of the static temperature and total temperature at the exit of the combustor, the combustion is more complete when the equivalence ratio is close to 1.0, and the total temperature and static temperature gradually reach the highest about 2750 K and 1800 K, respectively.

The airflow velocity and static temperatures at different equivalence ratios at the combustor exit are measured by TDLAS, and their relations with the time are shown in Figures 17 and 18, respectively. The results indicate that the change of the static temperature with the time can correspond to the four stages shown in Figure 8, and airflow velocity is the highest when the equivalence ratio is close to 1.0. It can be seen from the Figure 18 that the first stage is the initial airflow stage; the second stage is the hydrogen

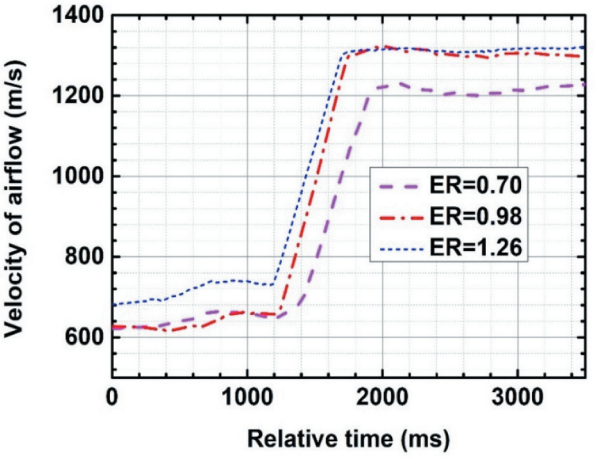

Figure 17. Velocity measured by TDLAS at different equivalence ratios.

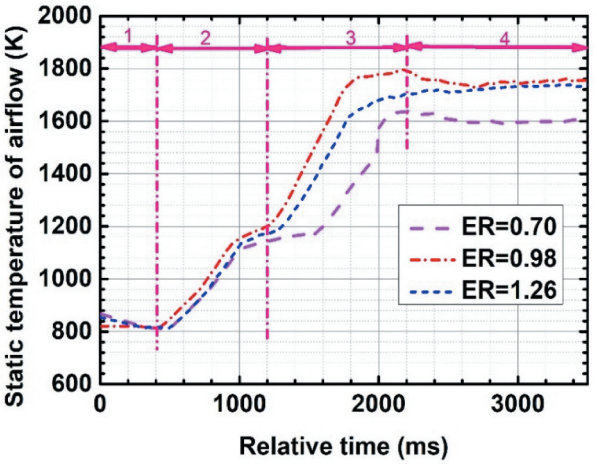

Figure 18. Static temperature measured by TDLAS of different equivalence ratios.

combustion stage that the temperature rises rapidly; the third stage is the combustion stage of both hydrogen and kerosene so that the temperature reaches maximum; and then the last stage is only kerosene combustion that the temperature decreases slightly. The comparisons of airflow velocity and temperature measured by TDLAS and that calculated by the one-dimension analysis method are shown in Figures 19 and 20. The results present that the deviations are less than 4% and −6%, respectively, which indicates the calculation is in great accordance with the TDLAS detections. The two percentages of 4% and −6% are based on the results of TDLAS, the degree of deviation between the one-dimensional calculation results and the test results.

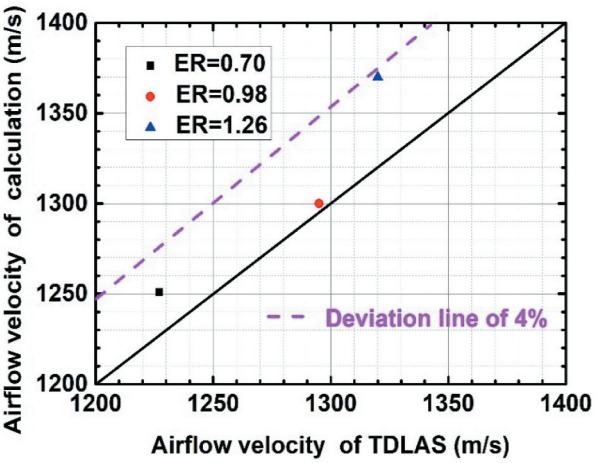

Figure 19. Airflow velocity of TDLAS measurement and one-dimensional calculation at different equivalence ratios at the combustor exit.

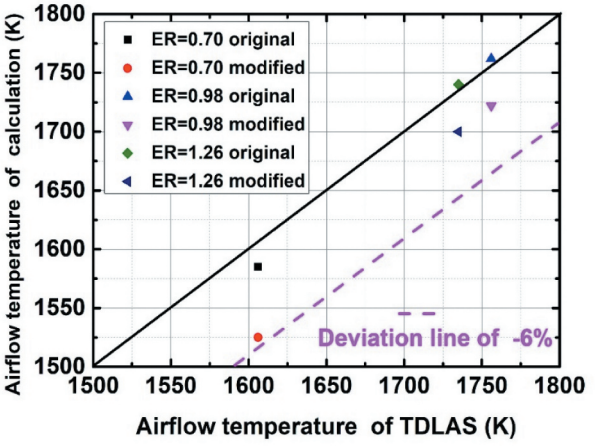

Figure 20. Airflow temperature of TDLAS measurement and one-dimensional calculation at different equivalence ratios at the combustor exit.

Concluding remarks

In this paper, mildly cracked (<10%) experiments of the *n*-dodecane were performed by a novel two-staged fuel heating system. The laminar flame speed and ignition delay time of the mildly cracking products of hydrocarbon fuels and surrogate gas fuel commonly used in the literature are compared, and it is found that there are significant differences between the two kinds fuel. Moreover, the supersonic combustion experiment of mildly cracked *n*-dodecane was carried out at Mach number 3.0 of combustor entrance with total temperature ~1550 K and total pressure ~1.5 MPa. The distributions of airflow velocity, static temperature, and total temperature along the axial direction of the combustor are calculated by using the one-dimensional analysis method with the measured static pressure along the axis

of combustor as the input. The calculated results are compared with the TDLAS detections at the combustor exit. The main conclusions are as follows:

(1) When the hydrocarbon fuel was mildly cracked, the cracked products contain a high proportion of large molecule hydrocarbons. From the calculation results, the presence of large molecule hydrocarbons affects the laminar flame speed and ignition delay time of the fuel. The ignition delay time of the mildly cracked products is about 50% higher than that of the surrogate gas fuel, and the laminar flame speed of the mildly cracked product is about 30% lower than that of the surrogate gas fuel. Therefore, when the hydrocarbon fuel was mildly cracked, the influence of large molecule hydrocarbons must be considered.
(2) The deviations of velocity and temperature of the airflow are less than 4% and −6%, respectively, which indicates the calculation is in great accordance with the TDLAS detection. The results provide useful experimental data for future numerical simulations.

Nomenclature

Q_F	Mass flowrate of Fuel
A*	Throat area of sonic flowmeter
T_F	Fuel temperature
p_F	Fuel pressure upstream sonic flowmeter
MF	Mole fraction
WF	Weight fraction
T_0	Total temperature
p_0	Total pressure
Q_{Air}	Air flowrate
p_{inj}	Fuel injection pressure
ER	Equivalence ratio

Acknowledgment

Thanks to Association professors Yang Lu and Kun Wu for the discussion.

Disclosure statement

No potential conflict of interest was reported by the author(s).

Funding

This work was sponsored by the Strategic Priority Research Program of Chinese Academy of Sciences [Grant No. XDA17030100], the Science and Technology Innovation Special Zone Project and National Key Project [Grant No. GJXM92579].

References

Denman, Z. J., V. Wheatley, M. K. Smart, and A. Veeraragavan. 2017. Supersonic combustion of hydrocarbons in a shape-transitioning hypersonic engine. *Proc. Combust. Inst.* 36 (2):2883–91. doi:10.1016/j.proci.2016.08.081.

Fan, X. J., G. Yu, J. G. Li, X. N. Lu, X. Y. Zhang, and C. J. Sung. 2007. Combustion and ignition of thermally cracked kerosene in supersonic model combustors. *J. Propuls. Power.* 23 (2):317–24. doi:10.2514/1.26402.

Fan, X. J., G. Yu, J. G. Li, L. J. Yue, X. Y. Zhang, and C. J. Sung. 2007. Effects of entry conditions on cracked kerosene-fueled supersonic combustor performance. *Combust. Sci. Technol.* 179 (10):2199–217. doi:10.1080/00102200701386198.

Fan, X. J., G. Yu, J. G. Li, X. Y. Zhang, and C. J. Sung. 2006. Investigation of vaporized kerosene injection and combustion in a supersonic model combustor. *J. Propuls. Power.* 22 (1):103–10. doi:10.2514/1.15427.

Gallo, E. C., L. Cantu, A. D. Cutler, R. D. Rockwell, C. P. Goyne, and J. C. Mcdaniel. 2015. WIDECARS measurements of a premixed ethylene-air flame in a small-scale dual-mode scramjet combustor.

Gascoin, N., G. Abraham, and P. Gillard. 2010. Synthetic and jet fuels pyrolysis for cooling and combustion applications. *J. Anal. Appl. Pyrolysis* 89 (2):294–306. doi:10.1016/j.jaap.2010.09.008.

Gokulakrishnan, P., C. Fuller, M. Klassen, Y. Zhu, D. F. Davidson, R. K. Hanson, and B. V. Kiel. 2016. Ignition of light hydrocarbon mixtures relevant to thermal cracking of jet fuels. 54th AIAA Aerospace Sciences Meeting. doi:10.2514/6.2016-0661.

Huang, B., U. Shrestha, R. J. Davis, and H. K. Chelliah. 2018. Endothermic pyrolysis of JP-10 with and without zeolite catalyst for hypersonic applications. *Aiaa J.* 56 (4):1616–26. doi:10.2514/1.J056432.

Huang, H., D. R. Sobel, and L. J. Spadaccini. 2002. Endothermic heat-sink of hydrocarbon fuels for scramjet cooling AIAA 2002-3871.

Ma, S. G., F. Q. Zhong, and X. Y. Zhang. 2018. Numerical study on supersonic combustion of hydrogen and its mixture with ethylene and methane with strut injection. *Int. J. Hydrogen Energy* 43 (15):7591–99. doi:10.1016/j.ijhydene.2018.03.007.

Nakaya, S., R. Kinoshita, J. Lee, H. Ishikawa, and M. Tsue. 2019. Analysis of supersonic combustion characteristics of ethylene/methane fuel mixture on high-speed measurements of CH* chemiluminescence. *Proc. Combust. Inst.* 37 (3):3749–56. doi:10.1016/j.proci.2018.09.011.

Nakaya, S., M. Tsue, M. Kono, O. Imamura, and S. Tomioka. 2015. Effects of thermally cracked component of n-dodecane on supersonic combustion behaviors in a scramjet model combustor. *Combust. Flame* 162 (10):3847–53. doi:10.1016/j.combustflame.2015.07.021.

Ravindran, M., M. Bricalli, A. Pudsey, and H. Ogawa. 2019. Mixing characteristics of cracked gaseous hydrocarbon fuels in a scramjet combustor. *Acta Astronaut.* 162:168–84. doi:10.1016/j.actaastro.2019.06.010.

Shin, J., and H. G. Sung. 2018. Combustion characteristics of hydrogen and cracked kerosene in a DLR scramjet combustor using hybrid RANS/LES method. *Aerosp. Sci. Technol.* 80:433–44. doi:10.1016/j.ast.2018.03.006.

Sirjean, B., E. Dames, D. A. Sheen, X. Q. You, and R. P. Lindstedt. 2008. A high-temperature chemical kinetic model of n-alkane oxidation, JetSurf version 1.0. *Chin. J. Nurs.*

Sun, M. B., X. D. Cui, H. B. Wang, and V. Bychkov. 2015. Flame flashback in a supersonic combustor fueled by ethylene with cavity flameholder. *J. Propuls. Power.* 31 (3):976–80. doi:10.2514/1.B35580.

Wang, Z., Y. S. Guo, and R. S. Lin. 2009. Pyrolysis of hydrocarbon fuel ZH-100 under different pressures. *J. Anal. Appl. Pyrolysis* 85 (1–2):534–38. doi:10.1016/j.jaap.2009.01.009.

Xian, X. C., G. Z. Liu, X. W. Zhang, L. Wang, and Z. T. Mi. 2010. Catalytic cracking of n-dodecane over HZSM-5 zeolite under supercritical conditions: experiments and kinetics. *Chem. Eng. Sci.* 65 (20):5588–604. doi:10.1016/j.ces.2010.08.004.

Yu, G., X. J. Fan, J. G. Li, L. J. Yue, and C. J. Sung. 2006. Experimental study on combustion of thermally-cracked kerosene in model supersonic combustors. 42nd AIAA/ASME/SAE/ASEE Joint Propulsion Conference & Exhibit.

Zhong, F. Q., L. W. Cheng, H. B. Gu, and X. Y. Zhang. 2019. Experimental study of flame characteristics of ethylene and its mixture with methane and hydrogen in supersonic combustor. *Aerosp. Sci. Technol.* 86:775–81. doi:10.1016/j.ast.2019.01.039.

Zhong, F. Q., X. J. Fan, G. Yu, and J. G. Li. 2009. Thermal cracking of aviation kerosene for scramjet applications. *Sci. China Ser. E-Technol. Sci.* 52 (9):2644–52. doi:10.1007/s11431-009-0090-8.